



Original scientific paper

## Preparation of mesoporous carbon/polypyrrole composite materials and their supercapacitive properties

WU-JUN ZOU, SHAN-SHAN MO, SHUANG-LI ZHOU, TIAN-XIANG ZHOU, NAN-NAN XIA and DING-SHENG YUAN✉

Department of Chemistry, Jinan University, Guangzhou 510632, China

✉Corresponding Author: E-mail: tydsh@jnu.edu.cn; Tel.: +86-20-85220597; fax: +86-20-85221697

Received: March 18, 2011; Revised: May 19, 2011; Published: August 20, 2011

---

### Abstract

We synthesized mesoporous carbons/polypyrrole composites, using a chemical oxidative polymerization and calcium carbonate as a sacrificial template.  $N_2$  adsorption-desorption method, Fourier infrared spectroscopy, and transmission electron microscopy were used to characterize the structure and morphology of the composites. The measurement results indicated that as-synthesized carbon with the disordered mesoporous structure and a pore size of approximately 5 nm was uniformly coated by polypyrrole. The electrochemical behavior of the resulting composite was examined by cyclic voltammetry and cycle life measurements, and the obtained results showed that the specific capacitance of the resulting composite electrode was as high as  $313 \text{ F g}^{-1}$ , nearly twice the capacitance of pure mesoporous carbon electrode ( $163 \text{ F g}^{-1}$ ). This reveals that the electrochemical performance of these materials is governed by a combination of the electric double layer capacitance of mesoporous carbon and pseudocapacitance of polypyrrole.

### Keywords

Mesoporous carbon/polypyrrole composites; Chemical oxidation; Calcium carbonate; Sacrificial template; Specific capacitance; Pseudocapacitance

---

### Introduction

Mesoporous carbon (MC) is one of the most important carbon materials with high surface area, uniform pore size, and good electric conductivity. During the past ten years, many efforts have been made to develop simple and efficient methods for the preparation of MC materials and to improve their properties for various applications. Recently, one-step soft template methods for MC preparation have gradually replaced time-consuming and tedious two-step hard mesoporous

silica templates, such as SBA-15, MCM-41, and MCM-48 [1,2]. The MCs and their composites are broadly applied to electrochemical capacitors [1,3], catalyst supports [4] and adsorbents [5,6], and magnetic separation [7]. Compared with mesoporous carbon materials, conducting polymers (CPs) possess pseudocapacitance, which is almost 10-100 times higher than the capacitance of electrochemical double-layer capacitors (EDLCs) [8]. Polypyrrole (PPy), one of CPs, has drawn a lot of attention for supercapacitor applications [9,10], mainly due to its oxidation-reduction properties, high conductivity in doped state, high specific capacitance, good environmental stability, and especially facile synthesis [11]. However, the shortcomings of CPs, such as low surface area and constrained power-output properties [12], markedly restrict their application to electrochemical capacitors. Hence, the most effective way is to use MC materials to improve the property of the CPs electrode. A new class of composite materials has originated from the combination of MCs and CPs [13]. Choi et al. introduced a conducting polymer layer into the pore surface of mesoporous carbon via vapor infiltration of a monomer and, by subsequent chemical oxidative polymerization, obtained mesoporous carbon-polypyrrole composites [14]. The maximum specific capacitance of these composites is  $274.5 \text{ F g}^{-1}$ . Pacheco-Catalán et al. synthesized mesoporous carbon/conducting polymer composites by adsorption of different monomers (aniline, pyrrole, thiophene, and 3-methylthiophene) in the gas phase onto the carbon surface, followed by oxidative chemical polymerization [15]. The electrochemical performance of carbon/polypyrrole composites electrode showed that it had a low specific capacitance (maximum value:  $83.8 \text{ F g}^{-1}$ ) and stable cycle life in the potential range of 0 to 1V. However, all those materials showed low specific capacitance. Recently, we prepared mesoporous carbon by one-step method [16]. The obtained results revealed that MCs display good capacitive behavior with high reversibility and reproducibility due to their unique large mesopore size, which is favorable for fast ionic transport. However, the specific capacitance of MCs reaches only  $163 \text{ F g}^{-1}$ , which limits their application to electric vehicles and high power electronic devices. In this study, we used PPy growth on the surface of MC via simple chemical oxidative polymerization with calcium carbonate as the sacrificial template to improve the capacitance of carbon materials. The resulting composite material combined double layer capacitance of MC with pseudocapacitance of PPy.

## Experimental

### Chemicals

Pyrrole monomer (98%, Aldrich Chemical Co.) was distilled under reduced pressure, transferred into a refrigerator, and stored under nitrogen until further use. The diameter of nanoscale calcium carbonate was 80 nm and the BET surface area was  $25 \text{ m}^2 \text{ g}^{-1}$ . Sodium 4-methyl benzene sulfonate (TsONa) was purchased from Sinopharm Chemical Reagent Co. Ltd, Shanghai, China. The other starting materials in this work were of analytical grade.

### Synthesis of mesoporous carbons/polypyrrole composites

MCs were synthesized from F127/silica/butanol according to the procedure described previously [16]. Typically,  $2 \text{ cm}^3$  sulfuric acid (98 wt%) and  $9.3 \text{ cm}^3$  butanol (BuOH) were directly added into a clear solution containing 2.5 g F127 and 120 g deionized water at 318 K. After stirring for 1.5 h,  $5 \text{ cm}^3$  tetraethyl orthosilicate (TEOS) was added, vigorously stirred at 318 K for 24 h, and aged at 373 K for 24 h. The F127/silica/butanol composites were collected by filtration and dried at room temperature for 12 h and at 433 K for 6 h. Finally, the obtained composites were transferred into a tube furnace and carbonized under pure  $\text{N}_2$  atmosphere at 1123 K for 2 h, followed by the treatment with diluted HF solution. The chemical oxidative polymerization of pyrrole was performed using a modified procedure reported previously [17]. First, 0.3 g TsONa, 0.5 g  $\text{CaCO}_3$ , 25 g  $\text{CaCl}_2$ ,  $20 \text{ cm}^3$   $\text{C}_2\text{H}_5\text{OH}$ , and 0.5 g Silica/Carbon were mixed into  $40 \text{ cm}^3$  deionized water with magnetic stirring under  $\text{N}_2$  atmosphere for 30 min; the nanoscale  $\text{CaCO}_3$  served as a

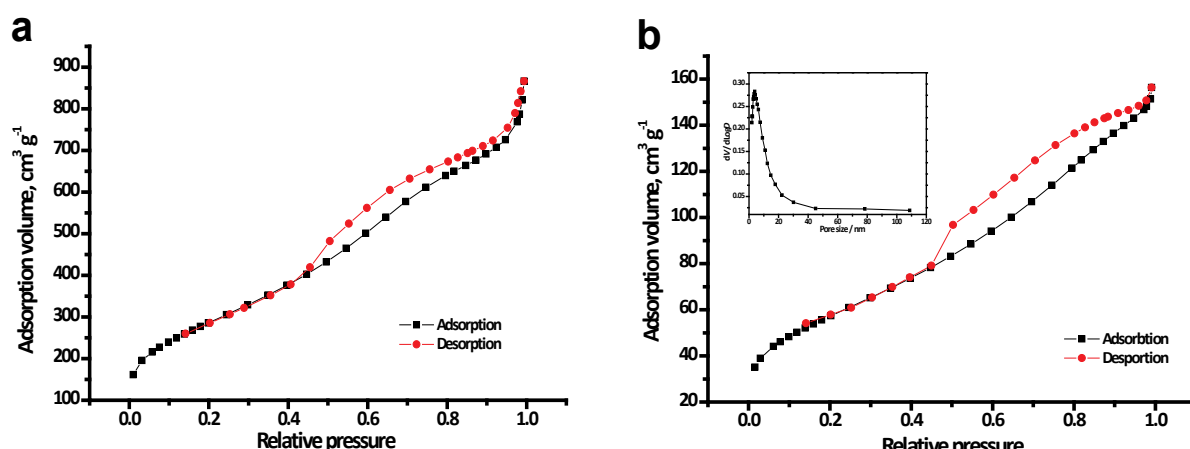
core, and TsONa was used as anionic surfactant. Then  $0.3 \text{ cm}^3$  pyrrole was added by a syringe. After 10 min,  $40 \text{ cm}^3$  of  $0.02 \text{ mol dm}^{-3}$   $\text{FeCl}_3$  solution was slowly added as oxidant into the reaction vessel. The polymerization was carried out for 12 h in an ice-bath with magnetic stirring and maintained under  $\text{N}_2$  atmosphere. The mesoporous carbon/polypyrrole composite was filtered and rinsed several times with distilled water and ethanol to remove retained pyrrole monomer and oxidant. The as-synthesized powder was transferred into HCl solution for  $\text{CaCO}_3$  removal for 24 h. The mixture was filtered and rinsed several times again with distilled water. Then the silica/carbon/PPy composite was treated by diluted HF solution to remove the silica and dried in vacuum at 333 K for 12 h. The product was denoted as MP, containing an approximate MC:PPy weight ratio of 6:4. Under the influence of the Lewis acid  $\text{FeCl}_3$  and inhibition by abundant  $\text{CaCl}_2$ ,  $\text{CaCO}_3$  was dissolved, slowly releasing  $\text{CO}_2$ , which contributed to the holes formation in the composite during the overflow process. Actually,  $\text{CaCO}_3$  as a core was the sacrificial template.

### Characterization

The morphologies of MC and as-synthesized composite were examined using a high-resolution transmission electron microscopy (TEM, JEOL JEM-2100, 200 kV). Nitrogen sorption isotherms of samples were measured by a Micrometrics TriStar 3000 analyzer at 77 K. The FT-IR measurements on samples were performed using Nicolet 6700 FT-IR spectrometer. The electrochemical behavior of both MC and MP was investigated by cyclic voltammetry (CV) conducted on a CHI 660 B electrochemical workstation (ChenHua Instruments Co., Shanghai, China). The measurements were carried out in a standard three-electrode cell system. A Pt-foil modified by either MC or MP was used as the working electrode, saturated calomel electrode was used as the reference electrode, and a Pt-foil as the auxiliary electrode. The working electrodes were prepared by mixing active materials (8 mg), acetylene black as a conductive reagent, and 5%-Nafion as a binder (80:10:10 wt %) and dispersed in absolute ethanol in ultrasonic bath. The dispersion was coated onto Pt foil drop by drop and then dried at 353 K. The CV experiments were carried out in aqueous solution of  $1 \text{ mol dm}^{-3}$   $\text{H}_2\text{SO}_4$ .

### Results and Discussion

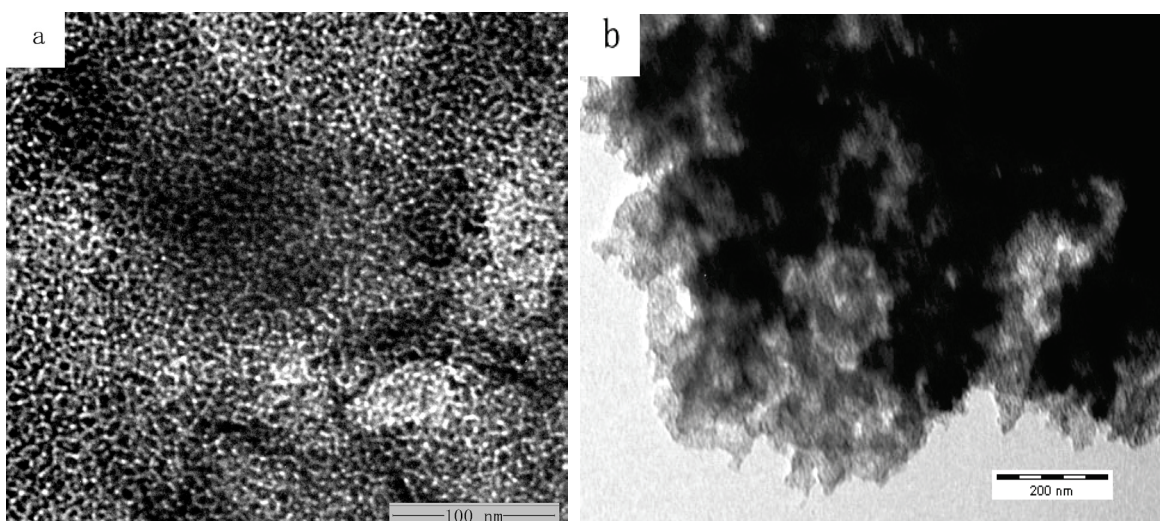
Fig. 1a and 1b show the  $\text{N}_2$  adsorption-desorption isotherms and BJH pore size distribution of MC and MP. The two samples are found to yield a type IV isotherm with a type H2 hysteresis loop near relative pressure of 0.50 in the desorption branch, which is associated with sharp capillary condensation taking place in mesopores [18].



**Figure 1.** Nitrogen adsorption-desorption isotherms and BJH pore size distribution (inset) of a) MC and b) MP.

The results show that the mesoporous structure of MC was maintained after loading of PPy. However, BET surface area of MP was considerably lower. The specific surface areas of mesoporous carbon and MP were  $1041\text{ m}^2\text{ g}^{-1}$  and  $207\text{ m}^2\text{ g}^{-1}$ , respectively (Table 1). The decrease of specific surface area is mainly attributed to the mesopores of the support being partially covered or filled by PPy. Therefore, pore volume and average pore size also decrease from  $1.18\text{ cm}^3\text{ g}^{-1}$  and  $5.2\text{ nm}$  to  $0.22\text{ cm}^3\text{ g}^{-1}$  and  $4.9\text{ nm}$ , respectively. This indicates that PPy was distributed evenly over the surface of MC.

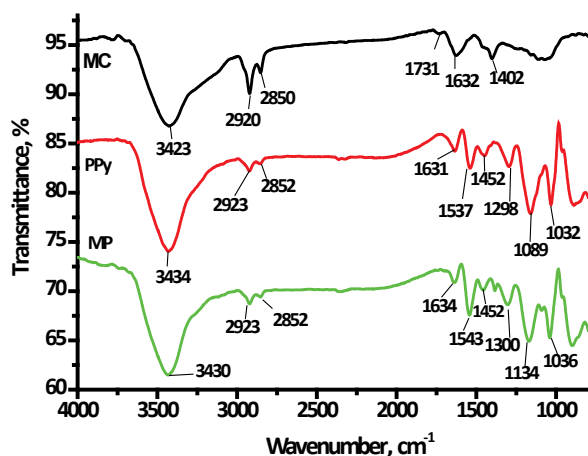
In order to gain further insights into the structure of mesoporous carbons, we investigated their appearance on the synthesized materials by TEM (Fig. 2). The disordered mesoporous size of MC with around  $5\text{ nm}$ , which is clearly visible in Fig. 2a, is in agreement with the data of the adsorption-desorption measurements (Fig. 1). Fig. 2b clearly shows the mesoporous structure of MC covered over with transparent films. In comparison with Fig. 2a, we may draw a conclusion that the transparent film is PPy and that it has been successfully loaded on the MC.



**Figure 2.** TEM images of **a)** MC and **b)** MP.

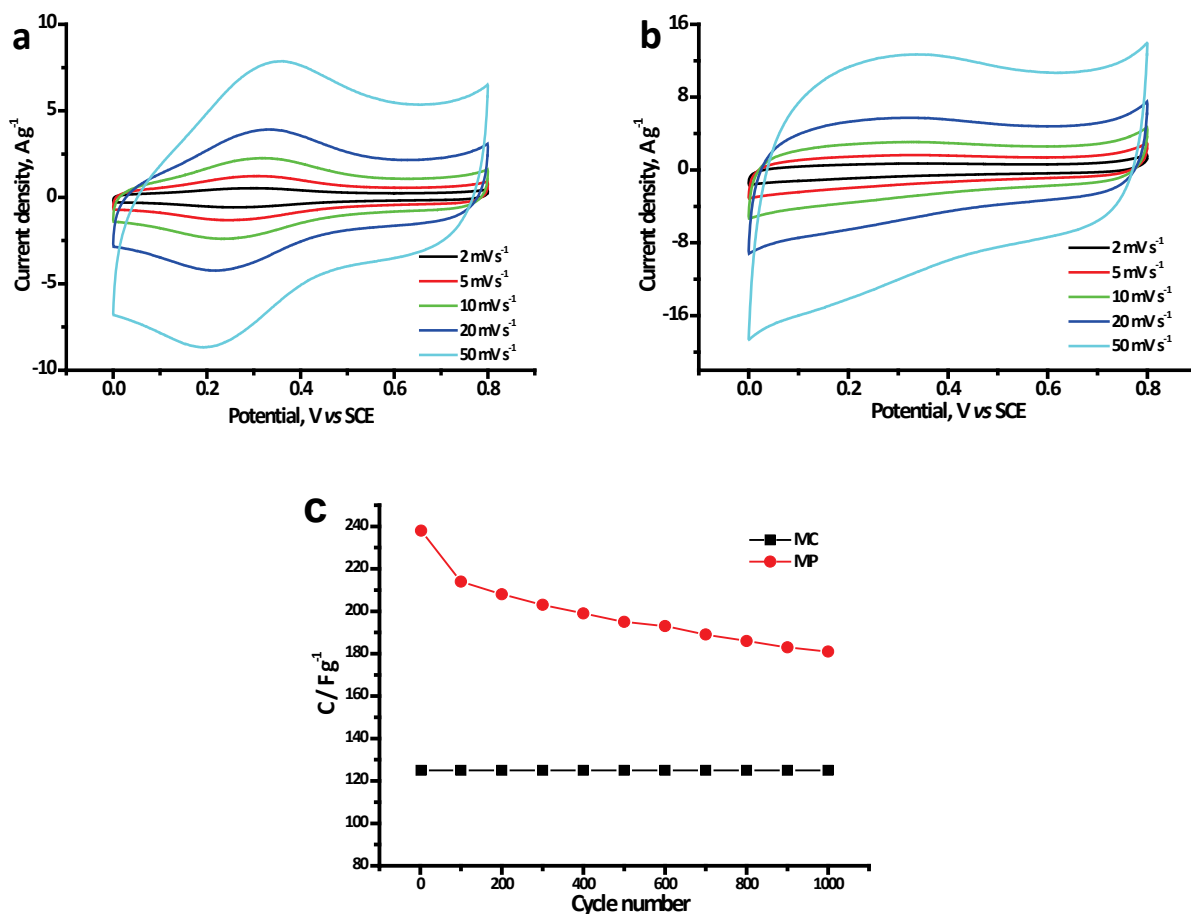
The functional groups of MC, PPy, and MP are characterized by FTIR spectroscopy (Fig. 3). The characteristic peak at  $3423\text{ cm}^{-1}$  is observed in the IR spectrum of MC and ascribed to  $-\text{OH}$ . The small peaks at  $2920$  and  $2850\text{ cm}^{-1}$  originate from the stretching vibrations of C–H bond. The peaks at  $1731$ ,  $1632$ , and  $1402\text{ cm}^{-1}$  could be assigned to the stretching vibration in carboxyl groups and C=O, C=C, and C–O bonds. The bands at  $1537$  and  $1452\text{ cm}^{-1}$  in PPy and MP spectra are due to the typical pyrrole ring vibration of pure PPy and bands of =C–H in plane vibration at  $1298$ ,  $1089$ , and  $1032\text{ cm}^{-1}$  [19]. The peaks at  $3434$  and  $1631\text{ cm}^{-1}$  correspond to N–H and C=C stretching vibrations, respectively. The spectrum of MP is very similar to that of PPy, verifying that PPy has been successfully applied onto MC. However, the peak at  $1632\text{ cm}^{-1}$  for C=O disappeared due to the combination of MC and PPy. Similarly, the peak for N–H stretching exhibits a red-shift phenomenon due to the interaction with the reactive hydroxyl functional groups [20].

Fig. 4 shows CVs of MC and MP in  $1\text{ mol dm}^{-3}\text{ H}_2\text{SO}_4$  at different scan rates. CVs of MC electrode contain redox peaks and deviate from the rectangular shape (Fig. 4a). With increasing scan rates, the redox current evidently increases, indicating that it has good rate capability. FTIR spectra confirm the existence of the abundant functional groups, for example C=O and O–H bonds, on the surface of MC. These groups are supposed to remarkably improve the hydrophilicity and wettability of the surface of MC and are beneficial for the aqueous electrochemical capacitors. The redox peaks might originate from the transformation of the O–H bond of MC into the C=O and *vice versa* during charge and discharge processes. In addition, the C=O bond of MC interacts with the  $\text{H}^+$  to become –OH in the reduced state, which would be re-oxidized into C=O during the discharge.



**Figure 3.** FT-IR spectra of MC, PPy and MP.

However, the CVs of MP present a steep increase in the current range from 0.0 to 0.1 V, which is an important behavior in supercapacitors [14], as shown in Fig. 4b. CV curves of the composites do not exhibit redox peaks as pronouncedly as in the case of MC. This is because the  $\pi$ -bonded surface of the MC may interact strongly with the conjugated structure of PPy, especially through the pyrrole ring [21], or N-H of PPy can interact with the reactive hydroxyl functional groups of MC [20].



**Figure 4.** CVs of **a)** MC and **b)** MP in  $1 \text{ mol dm}^{-3}$   $\text{H}_2\text{SO}_4$  electrolyte at different scan rates; **c)** cycle life of MC and MP in  $1 \text{ mol dm}^{-3}$   $\text{H}_2\text{SO}_4$  electrolyte at the scan rate of  $20 \text{ mV s}^{-1}$ .

The gravimetric specific capacitance ( $C$ ) of electrode is calculated according to the Eq. (1) from charge-discharge data of CVs:

$$C = \frac{Q}{WV} = \frac{\int idt}{W\Delta V} \quad (1)$$

where  $i$ ,  $W$  and  $V$  are the voltammetric current, the mass of active materials, and the total potential of electrochemical window, respectively. The calculated specific capacitances are listed in Table 1. The maximum specific capacitance of MP reaches as high as  $313 \text{ F g}^{-1}$  at the scan rate of  $2 \text{ mV s}^{-1}$ , which is nearly twice the specific capacitance of MC ( $163 \text{ F g}^{-1}$ ). Although the surface area of MC dramatically decreases due to the coverage of PPy, leading to the EDLC loss, the pseudocapacitance from the Faradic reaction on the PPy contributes much more to the total capacitance, leading to a higher specific capacitance of MP. Due to the different synthesis methods and electrolytes and measured potential windows, it is difficult to compare our results with those reported in the literatures. Therefore, for comparison purpose, we synthesized the PPy using the same method and measured the electrochemical properties in  $1 \text{ mol dm}^{-3} \text{ H}_2\text{SO}_4$ . The specific capacitance of pure PPy was  $328.4 \text{ F g}^{-1}$  at a scan rate of  $2 \text{ mV s}^{-1}$ . If the contribution of pure MC and pure PPy were calculated, the total was only  $229 \text{ F g}^{-1}$ . However, in this study, we obtained a higher result that reached  $313 \text{ F g}^{-1}$ , revealing the intensely synergistic effect between MC and PPy. Fig. 4c shows a cycle life of MC and MP in  $1 \text{ mol dm}^{-3} \text{ H}_2\text{SO}_4$  electrolyte at scan rate of  $20 \text{ mV s}^{-1}$ . The specific capacitance of MP drops from  $238 \text{ F g}^{-1}$  down to  $181 \text{ F g}^{-1}$  after 1000 cycles, corresponding to a 23.9% loss.

**Table 1.** Pore structure parameters of the MC and MP and the specific capacitances of MC and MP electrodes calculated from CVs in  $1 \text{ mol dm}^{-3} \text{ H}_2\text{SO}_4$  electrolyte

| Sample | Surface area<br>$\text{m}^2 \text{ g}^{-1}$ | Pore volume<br>$\text{cm}^3 \text{ g}^{-1}$ | Pore size<br>nm | $C / \text{F g}^{-1}$ |                       |                        |                        |                        |
|--------|---------------------------------------------|---------------------------------------------|-----------------|-----------------------|-----------------------|------------------------|------------------------|------------------------|
|        |                                             |                                             |                 | $2 \text{ mV s}^{-1}$ | $5 \text{ mV s}^{-1}$ | $10 \text{ mV s}^{-1}$ | $20 \text{ mV s}^{-1}$ | $50 \text{ mV s}^{-1}$ |
| MC     | 1041                                        | 1.18                                        | 5.2             | 163                   | 150                   | 139                    | 125                    | 103                    |
| MP     | 207                                         | 0.22                                        | 4.9             | 313                   | 281                   | 261                    | 238                    | 203                    |

## Conclusions

MC/PPy composites were successfully synthesized using a chemical method of oxidative polymerization. The resulting modified electrode showed some properties similar to the combination of the double layer capacitance of MC and pseudocapacitance of PPy. The results obtained by cyclic voltammetry demonstrated that the specific capacitance of the MP electrode was as high as  $313 \text{ F g}^{-1}$  compared to  $163 \text{ F g}^{-1}$  of MC electrode. In conclusion, it seems that the MP is a promising electrode material in supercapacitor field.

**Acknowledgements:** The study was financially supported by the National Natural Science Foundation of China (20876067 and 21031001) and the Fundamental Research Funds for the Central Universities (21609203).

## References

- [1] J. Lee, S. Yoon, T. Hyeon, S.M. Oh and K.B. Kim, *Chem. Commun.* **21** (1999) 2177-2178
- [2] K.T. Lee, X.L. Ji, M. Rault and L.F. Nazar, *Angew. Chem. Int. Ed.* **121** (2009) 5661-5665
- [3] J.X. Chen, N.N. Xia, T.X. Zhou, S.X. Tan, F.P. Jiang and D.S. Yuan, *Int. J. Electrochem. Sci.* **4** (2009) 1063-1073
- [4] S.H. Joo, S.J. Choi, I. Oh, J. Kwak, Z. Liu, O. Terasaki and R. Ryoo, *Nature* **412** (2001) 169-172
- [5] A. Vinu, C. Streb, V. Murugesan and M. Hartmann, *J. Phys. Chem. B* **107** (2003) 8297-8299

- [6] X.W. Liu, L. Zhou, J.W. Li, Y. Sun, W. Su and Y.P. Zhou, *Carbon* **44** (2006) 1386-1392
- [7] J.W. Lee, S.M. Jin, Y.S. Hwang, J.G. Park, H.M. Park and T. Hyeon, *Carbon* **43** (2005) 2536-2543
- [8] C. Peng, S.W. Zhang, D. Jewell and G.Z. Chen, *Prog. Nat. Sci.* **18** (2008) 777-788
- [9] X.Q. Lin and Y.H. Xu, *Electrochim. Acta* **53** (2008) 4990-4997
- [10] S.W. Woo, K. Dokko and K. Kanamura, *J. Power Sources* **185** (2008) 1589-1593
- [11] J. Wang, Y.L. Xu, X. Chen and X.F. Sun, *Compos. Sci. Technol.* **67** (2007) 2981-2985
- [12] W. Xing, X. Yuan, S.P. Zhuo and C.C. Huang, *Polym. Adv. Technol.* **20** (2009) 1179-1182
- [13] W. Xing, S. P. Zhuo, H.Y. Cui and Z.F. Yan, *Mater. Letters* **61** (2007) 4627-4630
- [14] M. Choi, B. Lim and J. Jang, *Macromol. Res.* **16** (2008) 200-203
- [15] D.E. Pacheco-Catalán, M.A. Smit, E. Morales, *Int. J. Electrochem. Sci.* **6** (2011) 78-90
- [16] X. Yan, H.H. Song and X.H. Chen, *J. Mater. Chem.* **19** (2009) 4491-4494
- [17] F.P. Jiang, T.X. Zhou, S.X. Tan, Y. Zhu, Y.L. Liu and D.S. Yuan, *Int. J. Electrochem. Sci.* **4** (2009) 1541-1547
- [18] K. S. W Sing, D. H. Everett, R. A. W. Haul, L. Moscou, R. A. Pierotti, J. Rouquerol and T. Simieniewska, *Pure Appl. Chem.* **57** (1985) 603
- [19] W. Chen, X.W. Li, G.Xue, Z.Q. Wang and W.Q. Zou, *Appl. Surf. Sci.* **218** (2003) 215-221
- [20] L. Ding, C. Hao, X.J. Zhang and H.X. Ju, *Electrochim. Commun.* **11** (2009) 760-763
- [21] Y.C. Zhao, X.L. Yang, J.N. Tian, F.Y. Wang and L. Zhan, *J. Power Sources* **195** (2010) 4634-4640

© 2011 by the authors; licensee IAPC, Zagreb, Croatia. This article is an open-access article distributed under the terms and conditions of the Creative Commons Attribution license

(<http://creativecommons.org/licenses/by/3.0/>) 